Cerebrovascular effects of endothelin-1 investigated using high-resolution magnetic resonance imaging in healthy volunteers

Anders Hougaard[1], Samaira Younis[1], Afrim Iljazi[1],
Kristian A Haanes[2], Ulrich Lindberg[3], Mark B Vestergaard[3],
Faisal M Amin[1], Kazutaka Sugimoto[4,5], Lars S Kruse[2,6],
Cenk Ayata[7] and Messoud Ashina[1]

Abstract
Endothelin-1 (ET-1) is a highly potent vasoconstrictor peptide released from vascular endothelium. ET-1 plays a major role in cerebrovascular disorders and likely worsens the outcome of acute ischaemic stroke and aneurismal subarachnoid haemorrhage through vasoconstriction and cerebral blood flow (CBF) reduction. Disorders that increase the risk of stroke, including hypertension, diabetes mellitus, and acute myocardial infarction, are associated with increased plasma levels of ET-1. The in vivo human cerebrovascular effects of systemic ET-1 infusion have not previously been investigated. In a two-way crossover, randomized, double-blind design, we used advanced 3 tesla MRI methods to investigate the effects of high-dose intravenous ET-1 on intra- and extracranial artery circumferences, global and regional CBF, and cerebral metabolic rate of oxygen ($CMRO_2$) in 14 healthy volunteers. Following ET-1 infusion, we observed a 14% increase of mean arterial blood pressure, a 5% decrease of middle cerebral artery (MCA) circumference, but no effects on extracerebral arteries and no effects on CBF or $CMRO_2$. Collectively, the findings indicate MCA constriction secondarily to blood pressure increase and not due to a direct vasoconstrictor effect of ET-1. We suggest that, as opposed to ET-1 in the subarachnoid space, intravascular ET-1 does not exert direct cerebrovascular effects in humans.

Introduction

Endothelin-1 (ET-1), a 21-amino acid peptide synthesized primarily by vascular endothelium, is one of the most potent human vasoconstrictors identified so far,[1] second only to urotensin-II.[2]

ET-1 plays a major physiologic role in regulating vascular function and blood flow in most organ systems, including the CNS, through activation of two receptor subtypes, ET_A and ET_B.[3] ET_A receptors are mainly expressed on vascular smooth muscle cells and causes vasoconstriction when activated, while ET_B receptors are primarily located on endothelial cells and their activation leads to vasodilation through release of nitric oxide.[3]

ET-1 plays a major role in cerebrovascular disorders. Marked increases of ET-1 levels in plasma[4] and

[1]Department of Neurology, Danish Headache Center, Rigshospitalet Glostrup, Glostrup, Denmark
[2]Department of Clinical Experimental Research, Rigshospitalet Glostrup, Glostrup, Denmark
[3]Department of Clinical Physiology, Functional Imaging Unit, Nuclear Medicine and PET, Rigshospitalet Glostrup, Glostrup, Denmark
[4]Department of Radiology, Massachusetts General Hospital, Harvard Medical School, Charlestown, USA
[5]Department of Neurosurgery, Yamaguchi University School of Medicine, Yamaguchi, Japan
[6]Department of Biochemistry, Rigshospitalet Glostrup, Glostrup, Denmark
[7]Stroke Service, Department of Neurology, Massachusetts General Hospital, Harvard Medical School, Charlestown, USA

Corresponding author:
Messoud Ashina, Department of Neurology, Danish Headache Center, Rigshospitalet Glostrup, Valdemar Hansens Vej 5, Glostrup DK-2600, Denmark.
Email: ashina@dadlnet.dk

cerebrovascular fluid[5] are seen after acute ischaemic stroke, potentially increasing ischaemic damage.[6] Following subarachnoid haemorrhage, ET-1 causes cerebral vasospasm and delayed ischaemic neurologic disturbances.[7] Studies in animal models indicate that these deleterious effects of ET-1 are caused by ET_A receptor activation.[6,8] In vitro studies of human cranial arteries have demonstrated ET_A receptor mediated contraction of cerebral, meningeal, and temporal arteries.[9] Interestingly, cerebral arteries may be more sensitive to ET-1 compared to arteries of other vascular beds.[10] In addition, disorders that increase the risk of stroke, including hypertension,[11] diabetes mellitus,[12] heart failure,[13] and acute myocardial infarction,[14] have been associated with increased plasma levels of ET-1. While the effects of systemically administered ET-1 on arterial pressure, heart rate, pulmonary and kidney function have been extensively studied in vivo in humans,[15–17] the in vivo effects on the human cerebrovascular system of acute and chronic plasma ET-1 level elevations are unknown.

In the present study, we used magnetic resonance imaging (MRI) at 3 T field strength to investigate the effects of intravenously administered ET-1 on intracranial (intracerebral, extracerebral) and extracranial arteries, using high-resolution time-of-flight angiography, and on regional and total brain perfusion as well as the global cerebral metabolic rate of oxygen ($CMRO_2$) in healthy human volunteers. We hypothesized that ET-1 infusion would decrease arterial circumferences and reduce global cerebral perfusion without changes in $CMRO_2$.

Methods

Participants

Healthy volunteers were recruited through announcement on a Danish website for recruitment of participants to health research (www.forsoegsperson.dk). Inclusion criteria were age 18–40 years and weight 50–100 kg. Exclusion criteria were (1) history of cardiovascular or cerebrovascular disease, diabetes, or hypercholesterolaemia, (2) ECG changes indicative of myocardial ischaemia or hypertrophy, (3) hypertension at baseline on an experimental day (defined as a systolic blood pressure above 150 mmHg or a diastolic blood pressure above 100 mmHg), (4) current pregnancy or breastfeeding, (5) daily intake of medication (except oral contraceptives), (6) daily smoking within last five years, (7) first-degree relatives with a history of myocardial infarction or stroke before the age of 65 years, (8) history of any primary headache disorders (except episodic tension-type headache for <2 days per month during the last year) or first-degree family members

with migraine as defined by the third International Classification of Headache Disorders.[18] Further, participants were excluded if there were any contraindications to MRI such as metal implants, pacemaker, insulin pump, claustrophobia, and/or surgical procedure during the last six weeks before inclusion.

The study was approved by the Ethical Committee of the Capital Region of Denmark (Protocol no. H-16022143). and conducted according to the Declaration of Helsinki and to the regulations of the Danish Data Protection Agency. The study is registered at ClincalTrials.gov (NCT 02906085). Written informed consent was obtained from all participants after detailed oral and written study information.

Experimental design

Participants received an intravenous infusion of ET-1 or placebo on two separate days, at least seven days apart, in a two-way crossover, randomized, double-blind design. All participants were headache-free for at least 72 h before each study day and the participants were not allowed use of caffeine or tobacco for 12 h before study start on each study day. Indwelling venous catheters (18G Vasofix® Safety, B.Braun, Melsungen, Germany) were inserted into both cubital veins: one for intravenous infusion and one for drawing blood samples. On each study day, participants underwent an MRI scan protocol consisting of two scan sessions: (1) a baseline MRI scan, followed by (2) an MRI scan during and following intravenous infusion (Figure 1).

On the ET-1 day, subjects received 8 ng/kg/min pharmaceutical grade ET-1 (CPC Scientific, Sunnyvale, USA) for 20 min. On the placebo day, the participants received isotonic saline infusion for 20 min. The randomization was done by the Hospital Pharmacy of the Capital Region of Denmark. Participants were instructed to remain still and avoid any head motion during the scan sessions.

Symptoms and vital signs

Participants were asked to report any perceived symptoms at −45, −33, −1, 15, 33, 45, and 60 min relative to the time of infusion start (T = 0). Since increased plasma ET-1 levels have previously been associated with migraine headache, we asked subjects specifically about the presence of head pain.[19] In case participants reported headache, headache characteristics (intensity, throbbing/constant pain, aggravation by activity, location, associated photo/phonophobia, nausea, or vomiting) were recorded using a standardized questionnaire. Headache intensity was recorded on a numerical rating scale (NRS 0–10) rating pain from none (NRS 0) to
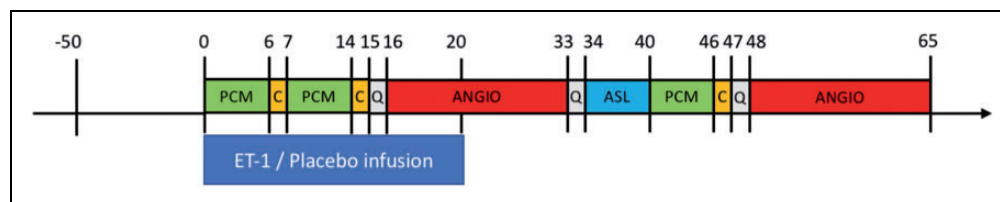
Figure 1. Overview of the study design and MR sequences. Subjects received infusions of ET-1 or isotonic saline (placebo) on two separate days in a randomized, double-blind crossover design. Numbers indicate time in minutes relative to the start of infusion (T = 0). Twelve subjects completed both study days. Of these, nine subjects underwent the second post-infusion angiography starting at T = 48. ANGIO: angiography; ASL: arterial spin labelling; C: $CMRO_2$ sequence; ET-1: endothelin-1; PCM: phase-contrast mapping for global mean CBF measurement; Q: scanning paused for questions about symptoms.

maximum imaginable (NRS 10). Vital signs were monitored during the experiments using an MR-compatible system (Veris Monitor, Medrad, Warrendale, PA). Heart rate, respiratory rate, blood oxygen saturation, nasal end-tidal CO_2 tension (water trap and gas sample line, Medrad, Warrendale, PA), and room temperature were continuously monitored and recorded every 5 s. Blood pressure was recorded every 5 min. For data analyses, all vital signs data were time-shifted for each participant relative to infusion start. Areas under the curves (AUCs) for all vital signs were calculated according to the trapezium rule for T = −20 to T = 0 (baseline) and for T = 0 to T = 60 (post-infusion). AUCs for the ET-1 days were compared to corresponding AUCs for the placebo days using paired t-tests. A two-sided probability level of less than 0.05 was considered statistically significant.

MRI data acquisition and data analysis

All MRI scans were performed on a 3.0 T Philips Achieva dStream MRI scanner (Philips Medical Systems, Best, The Netherlands) using a 32-channel phase array receive head coil.

High-resolution anatomical scans were obtained with a 3D T1-weighted turbo field echo sequence (field of view (FOV) = $240 \times 240 \times 170$ mm^3; voxel size = $1.00 \times 1.08 \times 1.10$ mm^3; echo time (TE) = 3.7 ms; repetition time (TR) = 8.0 ms; flip angle = 8°).

For all analyses, data analysts were blinded with respect to whether data were acquired on ET-1 days or placebo days.

MR angiography. A three-dimensional time-of-flight MR angiography (MRA) sequence was used for vessel imaging. First, we performed a scout MRA with the FOV $200 \times 200 \times 150$ mm^3, acquired matrix size 200×134, acquired voxel resolution $1.00 \times 1.50 \times 2.00$ mm^3, reconstructed resolution $0.39 \times 0.39 \times 1.00$ mm^3, TR 23 ms, TE 3.45 ms, flip angle 18°, SENSE p reduction 2, 2 chunks, duration 2 min 47 s. A subsequent scan to

record the MMA used FOV $200 \times 200 \times 37$ mm^3, acquired matrix size 800×570, acquired voxel resolution $0.25 \times 0.35 \times 0.70$ mm^3, reconstructed voxel resolution $0.20 \times 0.20 \times 0.35$ mm^3, TR 23 ms, TE 3.45 ms, flip angle 18°, SENSE p reduction 2.5, 3 chunks, duration 13 min 07 s. A scan to visualize the MCA specifically used FOV $200 \times 200 \times 12$ mm^3, acquired matrix size 784×572, acquired voxel resolution $0.26 \times 0.35 \times 0.70$ mm^3, reconstructed voxel resolution $0.20 \times 0.20 \times 0.35$ mm^3, TR 23 ms, TE 3.5 ms, flip angle 18°, SENSE p reduction 2.5, 1 chunk, duration 2 min 59 s.

After acquisition, data were transferred to a separate workstation in DICOM format and analysed by LKEB-MRA software.[20] The software operates by allowing the user to input start- and endpoint in a desired vessel, after which the software automatically detects the centre line and vessel contours perpendicular to this line. A circumference measurement is calculated for every 0.2 mm along the vessel segment. The segment was reviewed by the user and for each vessel a 5 mm (26 slices) sub-segment was chosen to ensure the most reliable measurement. If the chosen segment contained noisy or otherwise immeasurable slices, these slices were excluded from the segment. If the entire segment was immeasurable due to noise or artefacts, the segment was discarded altogether. The same sub-segment was chosen within each subject between scans and days. Measurements were performed bilaterally on the following vessels: middle cerebral artery (MCA), middle meningeal artery (MMA), superficial temporal artery (STA), internal carotid artery (ICA) (Figure 2).

To assess the effect of ET-1 administration on artery circumferences, we used a linear mixed model (equation (1)). Left–right averages ($Y_{art.circ}$) were modelled as the response parameter. Scan number (baseline, late-infusion scan, post-infusion scan – see Figure 1), day (ET-1 day, placebo day), and the interaction between those were included in the model as fixed effect with subject identification (u) and study day nested within
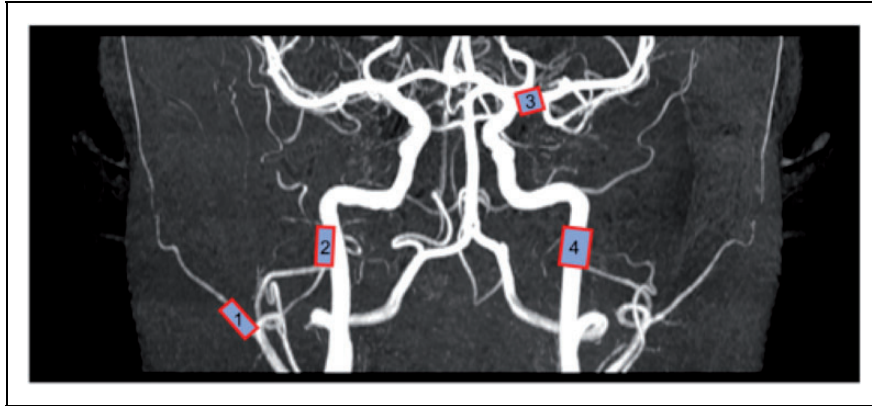
Figure 2. Locations of the examined segments of the superficial temporal (1), middle meningeal (2), middle cerebral (3), and internal carotid (4) arteries are marked.

subject identification as random effects to account for intra-subject variability

$$Y_{art.circ.} = \beta_0 + \beta_1 \cdot scan + \beta_2 \cdot drug + \beta_3 \cdot scan \\ \cdot drug + u + day : u + \varepsilon \quad (1)$$

The interaction term (β_3) describes significance of effect from ET-1 administration compared to placebo. The statistics was performed using Matlab (MathWorks, Natick, MA, USA) and statistical software package R (R Core Team http://www.R-project.org/, Vienna, Austria).

Arterial spin labelling (ASL). ASL was acquired using a 2D sequence with a pseudo-continuous labelling duration of 1650 ms followed by seven post-labelling delays ($TI_1/\Delta TI = 100$ ms/300 ms) acquired using a Look-Locker scheme with an echo planer imaging readout (13 axial slices; $FOV = 220 \times 220 \times 85$ mm^3; voxel size $= 3.44 \times 3.44 \times 6.6$ mm^3; $TR = 4000$ ms; $TE = 11$ ms; flip angle $= 40°$; slice readout duration $= 22$ ms). In addition, a proton density-weighted image was acquired with the same image resolution and matrix size as for the ASL image but with a TR of 10,000 ms.

Analysis of the ASL data was carried out using *oxford_asl*,[21] a part of FSL 5.0.10 (FMRIB Software Library, Functional Magnetic Resonance Imaging of the Brain Centre, Department of Clinical Neurology, University of Oxford, Oxford, UK).[22] Default values for pseudo-continuous ASL within *oxford_asl* were used adding only information of bolus duration, post-labelling delay, slice timing difference, and the Look-Locker flip angle. Quantification of the data was done using the recorded PD-weighted image also within *oxford_asl*.

The ASL data were registered to the MNI-152[23] standard 2 mm brain through a two-step procedure. First, the ASL data were registered using a boundary based registration (FLIRT, part of FSL) to the anatomical T1-weighted image. The T1-weighted image was then registered to the MNI-152 standard brain using a non-linear warp (FNIRT, part of FSL). Visual inspection of all registration steps was performed to assure good registration. Finally, in a voxel-wise general linear model using permutation-based non-parametric testing,[24] correcting for multiple comparisons across space by threshold-free cluster enhancement[25] (cluster-wise $P < 0.05$), we compared in a paired design (1) baseline ASL data to post-perfusion ASL data on ET-1 days and (2) changes in ASL data from baseline to post-perfusion on placebo days versus on ET-1 days. In addition, we specifically investigated CBF in regions of interest corresponding to the arterial territories of the brain based on a previously developed atlas.[26]

Phase-contrast mapping (PCM). Mean global CBF was measured by acquiring the blood flow in the carotid arteries and basilar artery using PCM MRI technique.[27,28] Blood velocity maps were acquired using a turbo field echo sequence (1 slice; $FOV = 240 \times 240$ mm^2; voxel size $= 0.75 \times 0.75 \times 8$ mm^3; $TE = 7.33$ ms; $TR = 27.63$ ms; flip angle $= 10°$; velocity encoding $= 100$ cm/s, without cardiac gating). Three measurements were acquired with the imaging planes placed orthogonal to each of the carotid arteries or the basilar artery, respectively. The total blood flow to the brain was obtained by drawing regions of interest (ROIs) covering the arteries and multiplying the mean blood velocity by the cross-sectional area of each ROI. ROIs were initially drawn on the phase-magnitude images and then transferred to the velocity maps. All processing was performed using Matlab scripts developed in-house. Quantitative global CBF values were calculated by normalizing the total blood flow to the brain weight. Brain weight was estimated from the anatomical scan using FSL BET and FAST software

(parts of the FSL software package, see above) and assuming a brain density of $1.05\,g/ml$.[29] The oxygen saturation of the venous blood leaving the sagittal sinus was acquired using susceptibility-based oximetry (SBO) MRI technique.[30] The global $CMRO_2$ could then be calculated by multiplying the haemoglobin concentration, the CBF acquired by PCM, and the arterio-venous oxygen saturation difference of the brain (Fick's principle). SBO utilizes that the different magnetic susceptibility of oxygenated and deoxygenated haemoglobin can be related to oxygen saturation using the model described by Rodgers et al.[31] Magnetic susceptibility-weighted maps were acquired using a dual-echo gradient-echo sequence (1 slice, $FOV = 220 \times 190$ mm^2, voxel size $= 0.5 \times 0.5 \times 8$ mm^3, TE 1 $= 10.9\,ms$, TE 2 $= 24.2\,ms$, flip angle $= 30°$, five repeated measures, total duration $= 1\,min\,30\,s$, SENSE-factor $= 2$). The imaging slice was located orthogonal to the sagittal sinus. Aliased phase-values were unwrapped manually if necessary. The magnetic susceptibility of blood in the sagittal sinus and tissue was obtained by drawing regions of interests. In-depth discussion of the post processing has been described earlier.[32] All processing was performed using Matlab scripts developed in-house. To assess the effect of ET-1 administration on CBF and $CMRO_2$ a linear mixed model, similar to the model described in equation (1), was applied.

Blood samples

Blood samples were drawn at baseline and at 20 min following start of infusion from the indwelling venous cannula positioned in the forearm not being used for infusion of ET-1 or saline. Samples were anticoagulated with EDTA and spun for 10 min at 3500 r/min at 4°C to obtain plasma, which was stored immediately at $-80°C$. The ET-1 concentration in each sample was subsequently determined using a Quantikine® ELISA kit from R&D Systems (#DET100) according to the manufacturer's recommendations using the kit-provided ET-1 standard (synthetic human ET-1) and a Quantikine® ELISA kit control set containing recombinant human ET-1 in three different concentrations (#QC82, R&D Systems) as positive control. All samples were initially diluted 1:2 before assaying except for the infusion liquid which was diluted 1:25,000. For samples exceeding the highest standard, further serial dilutions were performed until they were within the range of the standard series. All samples were run in duplicate and mean concentration (pg/ml) was used for calculations.

Results

In total, 14 healthy subjects (eight women, mean age 26.1 years, SD 4.7 years) were included. One subject withdrew from the study after the first study day (ET-1 infusion) due to discomfort (mild claustrophobia) experienced during the MRI procedure. Another subject was only scanned on the placebo day due to technical problems on the ET-1 day. During infusion, four subjects reported mild nausea and another subject reported headache (NRS 1) on the ET-1 day, while one subject reported headache (NRS 1) on the placebo day. One subject reported headache (up to NRS 7) occurring 2 h after discharge, lasting for 1 h, on the placebo day. No other adverse events were observed or reported during or up to 24 h after the experiment.

Neuroradiologist review of the images revealed a cholesterol granuloma in one subject, a pituitary adenoma (8 mm) in a second subject, and a pineal gland cyst (largest dimension 15 mm) in a third subject. These subjects underwent appropriate further investigations and none of them required any form of intervention. The observed abnormalities were unlikely to affect the vascular measures of the present study.

Vital signs

Baseline AUCs were not different between ET-1 days and placebo days for any of the recorded vital signs. AUCs for systolic and diastolic arterial blood pressure increased significantly following ET-1 infusion compared to placebo infusion while the area under the curve for heart rate decreased ($P < 0.001$, see Figure 3). No differences were found for respiratory rate, blood oxygen saturation, and nasal end-tidal CO_2 tension. Room temperatures did not differ between baseline and ET-1 days (baseline days mean 20.5°C (SD 0.4°C), ET-1 days mean 20.6°C (SD 0.4°C).

MRA

Nine of the subjects underwent a third angiography at $T = 48\,min$. Two subjects had an MMA on one side only (a commonly seen anatomical variant). In some cases, the MCA was not sufficiently visualized to allow for accurate measurements, likely due slight subject head movement causing the MCA to move outside of the narrow high-resolution FOV used for MCA acquisition. For the MCA, 24 of 26 angiographies were included at baseline, 21 of 26 at scan 1, and 11 of 15 at scan 2. Bilateral angiographies of the STA and ICA were included for all subjects and for all scans. Results from the mixed linear model, taking into account arterial circumference variation on both experimental days, showed reduction of MCA circumference from baseline (mean 9.01 mm, SD 0.69 mm) to the second post-infusion angiography, i.e. scan 2 (mean 8.53 mm, SD 0.50 mm, $P = 0.026$) on the ET-1 day. MCA circumference was not significantly changed
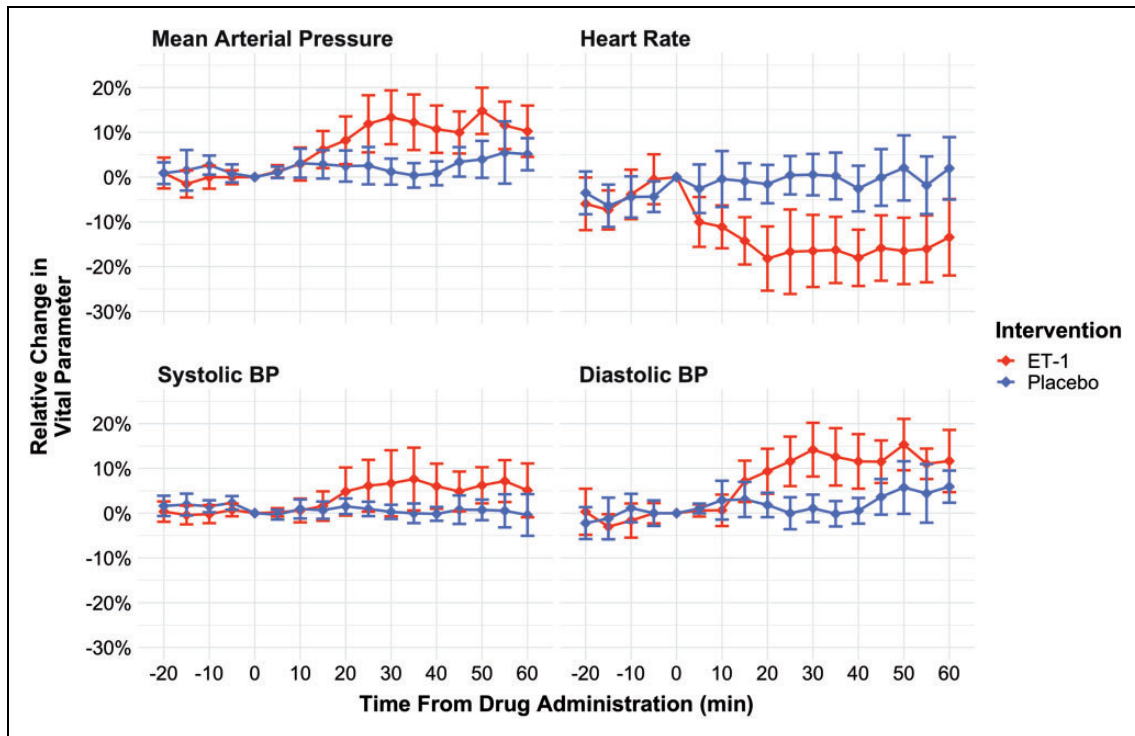
Figure 3. Vital signs (non-invasive systolic, diastolic, and mean arterial blood pressure, and heart rate) during the study. Red lines: ET-1 infusion days, blue lines: placebo infusion days Values are means of all participants. Error bars indicate the 95% confidence intervals of the mean. ET-1: endothelin-1.

from baseline at scan 1 (mean 8.63 mm, SD 0.68 mm, $P = 0.137$). No MCA changes were observed on the placebo day and no changes of the MMA, STA, or ICA were observed on any of the experimental days (see Figure 4). Circumferences for MMA on the ET-1 day were 4.90 (SD 0.67 mm) at baseline, 5.26 mm (SD 0.57 mm) at scan 1, and 5.08 mm (SD 0.68 mm) at scan 2. For STA, 6.01 mm (SD 0.68 mm) at baseline, 6.52 mm (SD 0.91 mm) at scan 1, and 6.80 mm (SD 1.20 mm) at scan 2. For ICA, 15.13 mm (SD 1.29 mm) at baseline, 14.92 mm (SD 1.43 mm) at scan 1, and 15.00 mm (SD 1.63 mm) at scan 2.

ASL and PCM

We found no changes from baseline of global mean CBF or $CMRO_2$ at any time after ET-1 infusion (mean baseline global CBF: 58.44 ml/100 g/min (SD 5.87 ml/100 g/min)), mean post-infusion global CBF (average of all three measurements): 57.70 ml/100 g/min (SD 5.32 ml/100 g/min), mean baseline total $CMRO_2$: 153.12 μmol/min/100 g (SD 43.04 μmol/min/100 g), mean post-infusion global CBF (average of all three measurements): 150.88 μmol/min/100 g (SD 39.98 μmol/min/100 g). The voxel-wise ASL analyses did not show any changes from baseline of regional CBF after ET-1 infusion.

Blood samples

The average baseline plasma concentration of ET-1 was 1.64 pg/ml (SD 0.86 pg/ml, range: 0.12–3.66 pg/ml). On the ET-1 day, the concentration increased from 1.78 pg/ml at baseline to 92.25 pg/ml after 15 min infusion ($P = 0.01$, paired t-test). A marked increase of ET-1 concentration was observed in all subjects. On the placebo day, the concentration was 1.51 pg/ml at baseline and 1.61 pg/ml following 15 min infusion ($P = 0.76$, paired t-test).

Discussion

We conducted the first in vivo human study of the effects of systemic ET-1 administration on cranial arterial circumference, cerebral blood flow (CBF), and cerebral oxygen metabolism. We found a moderate constriction of the MCA but no effects on regional or global CBF or total $CMRO_2$ following ET-1 infusion.

Several previous studies in animals have investigated the in vivo cerebrovascular effects of ET-1. A study of repeated cerebral angiographies in cats and dogs reported marked constriction of the basilar artery when ET-1 was administered intracisternally, while no constriction was found after intra-arterially administered ET-1.[33] The authors suggested, as an explanation
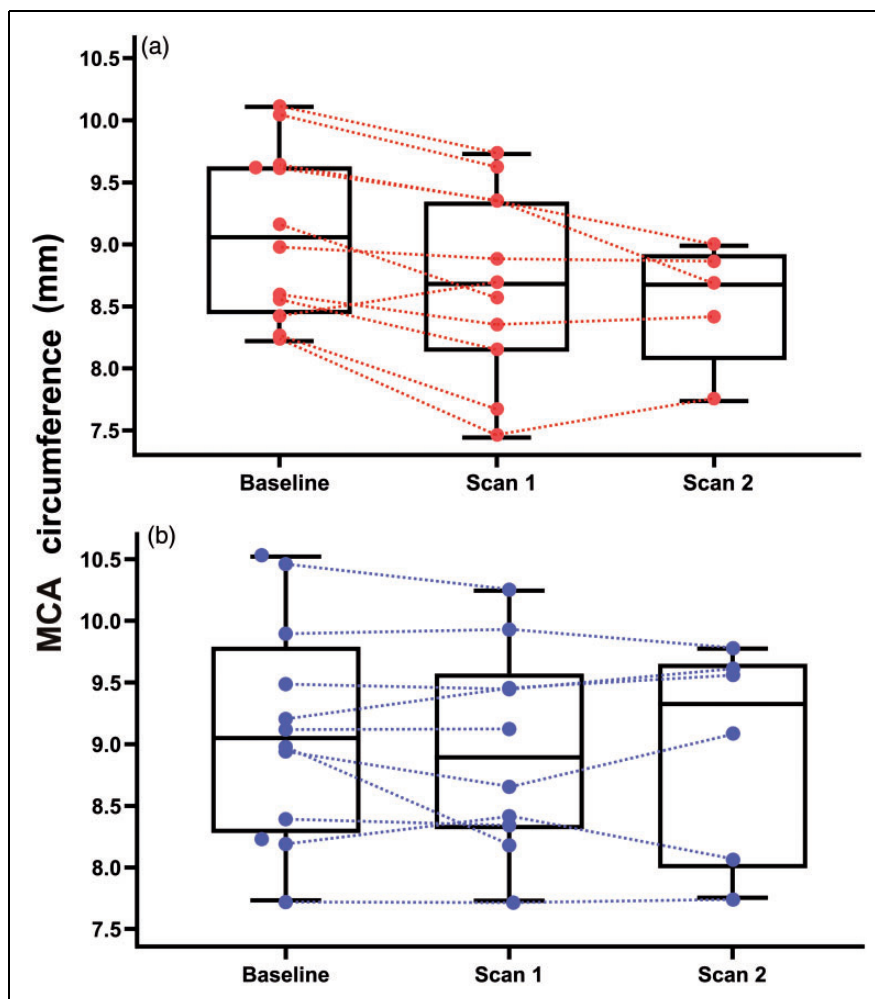
Figure 4. Combined box and dot plots of arterial circumferences of the MCA (mm, left–right average) at baseline, during scan 1 (MRA acquired from T = 16 to T = 33), and during scan 2 (MR angiography acquired from T = 48 to T = 65). (a) ET-1 infusion day and (b) placebo (isotonic saline) infusion day. MCA: middle cerebral artery.

of these findings, that ET-1 is not able to cross the tight junctions of the cerebrovascular endothelium, the 'blood–arterial wall barrier', and reach its receptor on the vessel wall smooth muscle cells. Likely, if ET-1 could cross the blood–brain barrier and reach the cerebrospinal fluid, it would exert a vasoconstrictive effect from the abluminal side. In support, an autoradiographic study using intravenous ^{125}I-labeled ET-1 showed no distribution of ET-1 into the CNS in rats, except for areas known to lack a blood–brain barrier.[34]

The observation that abluminal ET-1 potently constricts cerebral arteries in vivo has been reproduced in several studies,[35,36] and this effect is currently used in a well-established animal model of ischaemic stroke.[37] Similarly, intravascular ET-1 did not produce changes in CBF in studies of squirrel monkeys[38] and rabbits.[39] However, in one study, ET-1 infused into the internal maxillary artery of unanaesthetized goats produced dose-dependent sustained decreases in CBF.[40]

The observation in the present study of a moderate decrease of MCA circumference can be explained either by a direct vasoconstrictor effect of intravascular ET-1 or an effect secondary to the ET-1 induced changes in arterial blood pressure through autoregulation. If MCA constriction was due to a direct effect of ET_A receptor activation, it is puzzling that similar effects were not seen in the MMA and the STA, since ET_A receptors are equally present in these arteries.[9] In addition, the lack of CBF changes, even in areas supplied by MCA, suggests an autoregulatory effect. Further, previous studies of intravenously administered vasoactive peptides acting on smooth muscle receptors in vivo in humans indicate a specific effect on extracerebral (STA, MMA) and not intracerebral (MCA) arteries,[41,42] presumably due to the blood–brain barrier. Currently, only few studies have assessed the relationship between changes in blood pressure and diameter of the MCA.[43,44] In a human in vivo

craniotomy study, the ACA and M2 segment of the MCA dilated 25% whereas the M1 segment of the MCA was unaffected during large alterations in blood pressure (range of 30 mmHg) induced by nitroprusside and phenylephrine infusion.[45] In a 1.5 T MRI angiography study in healthy humans, the M1 segment of the MCA was unchanged during moderate hypotension.[46]

In the present study, we observed increases of arterial blood pressure following ET-1 infusion (8 ng/kg/min for 20 min). At T = 30 min, diastolic blood pressure had increased by approximately 14% and systolic blood pressure by approximately 7% compared to T = 0 (Figure 3.). Previous studies of intravenous ET-1 infusion in healthy humans reported comparable results. Infusion of increasing ET-1 doses of 1.0, 2.5, 5.0 ng/kg/min for 15 min each resulted in an increase of mean arterial blood pressure of 6.3% at 45 min post-infusion start relative to baseline.[16] Infusion of 0.75 pmol/kg/min (1.9 ng/kg/min) for 30 min, then increased to 1.5 pmol/kg/min (3.7 ng/kg/min) for 30 min and then to 3.0 pmol/kg/min (7.5 ng/kg/min) for a further 30 min resulted in a 17.5% increase in diastolic blood pressure and a 5.6% increase in systolic blood pressure at 90 min post-infusion start compared to infusion start. The blood pressure increase is presumably due to constriction of resistance vessels.[3] Likewise, ET-antagonism in healthy humans reduces peripheral resistance (with concomitant reduction primarily of diastolic blood pressure).[47] Collectively, the observed MCA constriction in the present study is most likely an autoregulatory effect secondary to an increase in arterial blood pressure, and not a direct effect of ET-1 on vascular ET-receptors.

Although we used the highest concentration of ET-1 administered to human subjects, we cannot rule out that a more pronounced effect on cerebral arteries, and a reduction in CBF, would have been seen at higher dosages. Also, the effects may theoretically have been different in patients with, e.g. severe hypertension or compromised cerebral autoregulation.

Increases of plasma ET-1 levels are seen in numerous disorders.[3] Based on the findings of the present study, it seems clear that even very high acute increases in systemic ET-1 levels (exceeding those seen in, e.g. acute myocardial infarction[14]) do not affect CBF or oxygen metabolism. Consequently, endothelin antagonists are unlikely to have a clinically relevant protective effect on neurovascular function in conditions associated with elevated systemic ET-1 levels.

Conditions associated with leakage of intravascular ET-1 to the abluminal side of cerebral arteries, e.g. subarachnoid haemorrhage, may be associated with ET-1-mediated vasoconstriction. However, the source of ET-1-induced vasoconstriction after subarachnoid haemorrhage is most likely primarily the vascular endothelium, due to arterial damage, rather than ET-1 circulating in the vascular system. Notably, while endothelin-receptor antagonists significantly reduce angiographic vasospasm following aneurismal subarachnoid haemorrhage, they have not been shown to reduce mortality or to prevent an unfavourable outcome (either death or dependency) in this condition.[48]

ET-1 has been suggested to be an endogenous trigger of migraine aura and migraine headache.[19] In the present study, none of the subjects reported migraine aura symptoms. Previous studies demonstrated potent induction of spreading depolarization, the pathophysiological phenomenon likely underlying the migraine aura,[49] following brain topical application of ET-1 in animals via ET_A receptor activation.[50,51] These studies suggested that ET-1 could be the cause of migraine aura in cases where an endothelial irritation is suspected to trigger the aura.[50] The source of ET-1 according to this hypothesis would not be intraluminal ET-1 but abluminally secreted ET-1 from the endothelium. Further, the likely reason for ET-1 induced spreading depolarization in animal models is the induction of an area of micro-ischaemia.[52] Therefore, based on this hypothesis, the absence of migraine aura symptoms following intravenous ET-1 infusion is not surprising. Another hypothesis concerning migraine aura and ET-1 is based on the observation of migraine aura-like symptoms as an adverse effect of sclerotherapy for the treatment of varicose veins,[53] which has been proposed to be mediated by an increase of intravascular ET-1 levels caused by the sclerosant agent.[54] Average increases of ET-1 levels following polidocanol sclerotherapy were 24%,[54] i.e. much less than the more than 50-fold increase observed in the present study.

Likewise, in the present study, ET-1 did not produce more headache than placebo. Interestingly, other vasoconstricting agents, norepinephrine[55] and prostaglandin $F_{2\alpha}$,[56] also did not cause headache in healthy subjects. While ET-1 infusion does not cause migraine symptoms in healthy subjects, we cannot rule out that this would be the case in genetically susceptible individuals, i.e. migraine patients.[19]

In conclusion, we found a pronounced increase in arterial blood pressure and a moderate reduction of MCA circumference following intravenous ET-1 infusion in healthy volunteers, but no changes of extracerebral artery circumference, or of CBF or $CMRO_2$. We suggest that the observed MCA constriction is due to an autoregulatory effect secondary to blood pressure increase and not a direct vasoconstrictor effect of ET-1 on cerebral arteries. Thus, as opposed to ET-1 in the subarachnoid space, intravascular ET-1 does not seem to exert direct cerebrovascular effects in healthy humans.

Declaration of conflicting interests

The author(s) declared no potential conflicts of interest with respect to the research, authorship, and/or publication of this article.

Data availability

Original data from the study can be obtained from the corresponding author upon reasonable request.

Authors' contributions

AH and MA conceived and designed the study. AH, SY, AI, KAH, and LSK conducted the MRI experiments and/or laboratory analyses. AH, UL, MBV, and FMA analysed the data, and drafted the manuscript. SY, AI, KAH, KS, LSK, and CA contributed to data analysis and data interpretation and revised the manuscript critically for important intellectual content. All authors approved the final version of the manuscript.

ORCID iD

Kristian A Haanes https://orcid.org/0000-0001-5182-8957

References

1. Yanagisawa M, Kurihara H, Kimura S, et al. A novel potent vasoconstrictor peptide produced by vascular endothelial cells. *Nature* 1988; 332: 411–415.
2. Ames RS, Sarau HM, Chambers JK, et al. Human urotensin-II is a potent vasoconstrictor and agonist for the orphan receptor GPR14. *Nature* 1999; 401: 282–286.
3. Davenport AP, Hyndman KA, Dhaun N, et al. Endothelin. *Pharmacol Rev* 2016; 68: 357–418.
4. Ziv I, Fleminger G, Djaldetti R, et al. Increased plasma endothelin-1 in acute ischemic stroke. *Stroke* 1992; 23: 1014–1016.
5. Franceschini R, Gandolfo C, Cataldi A, et al. Twenty-four-hour endothelin-1 secretory pattern in stroke patients. *Biomed Pharmacother* 2001; 55: 272–276.
6. Patel TR, Galbraith S, Graham DI, et al. Endothelin receptor antagonist increases cerebral perfusion and reduces ischaemic damage in feline focal cerebral ischaemia. *J Cereb Blood Flow Metab* 1996; 16: 950–958.
7. Suzuki R, Masaoka H, Hirata Y, et al. The role of endothelin-1 in the origin of cerebral vasospasm in patients with aneurysmal subarachnoid hemorrhage. *J Neurosurg* 1992; 77: 96–100.
8. Vergouwen MDI, Algra A and Rinkel GJE. Endothelin receptor antagonists for aneurysmal subarachnoid hemorrhage. *Stroke* 2012; 43: 2671–2676.
9. Adner M, Jansen I and Edvinsson L. Endothelin – a receptors mediate contraction in human cerebral, meningeal and temporal arteries. *J Auton Nerv Syst* 1994; 49: S117–21.
10. Fukuda S, Taga K and Shimoji K. High sensitivity of porcine cerebral arteries to endothelin. *Experientia* 1991; 47: 475–477.
11. Dhaun N, Goddard J, Kohan DE, et al. Role of endothelin-1 in clinical hypertension: 20 years on. *Hypertension* 2008; 52: 452–459.
12. Donatelli M, Colletti I, Bucalo ML, et al. Plasma endothelin levels in NIDDM patients with macroangiopathy. *Diabetes Res* 1994; 25: 159–164.
13. Stewart DJ, Cernacek P, Costello KB, et al. Elevated endothelin-1 in heart failure and loss of normal response to postural change. *Circulation* 1992; 85: 510–517.
14. Stewart DJ, Kubac G, Costello KB, et al. Increased plasma endothelin-1 in the early hours of acute myocardial infarction. *J Am Coll Cardiol* 1991; 18: 38–43.
15. Kiely DG, Cargill RI, Struthers AD, et al. Cardiopulmonary effects of endothelin-1 in man. *Cardiovasc Res* 1997; 33: 378–386.
16. Vierhapper H, Wagner O, Nowotny P, et al. Effect of endothelin-1 in man. *Circulation* 1990; 81: 1415–1418.
17. Sørensen SS, Madsen JK and Pedersen EB. Systemic and renal effect of intravenous infusion of endothelin-1 in healthy human volunteers. *Am J Physiol* 1994; 266: F411–F418.
18. Headache Classification Committee of the International Headache Society (IHS). The International Classification of Headache Disorders, 3rd edition. *Cephalalgia* 2018; 38: 1–211.
19. Iljazi A, Ayata C, Ashina M, et al. The role of endothelin in the pathophysiology of migraine – a systematic review. *Curr Pain Headache Rep* 2018; 22: 713.
20. Amin FM, Lundholm E, Hougaard A, et al. Measurement precision and biological variation of cranial arteries using automated analysis of 3 T magnetic resonance angiography. *J Headache Pain* 2014; 15: 25.
21. Chappell MA, Groves RA, Whitcher B, et al. Variational Bayesian inference for a non-linear forward model. *IEEE Trans Signal Processing* 2009; 57: 223–236.
22. Jenkinson M, Beckmann CF, Behrens TEJ, et al. FSL. *Neuroimage* 2012; 62: 782–790.
23. Grabner G, Janke AL, Budge MM, et al. Symmetric atlasing and model based segmentation: an application to the hippocampus in older adults. *Med Image Comput Comput Assist Interv* 2006; 9: 58–66.
24. Nichols TE and Holmes AP. Nonparametric permutation tests for functional neuroimaging: a primer with examples. *Human Brain Mapping* 2002; 15: 1–25.
25. Smith SM and Nichols TE. Threshold-free cluster enhancement: addressing problems of smoothing,

threshold dependence and localisation in cluster inference. *Neuroimage* 2009; 44: 83–98.

26. Kabir Y, Dojat M, Scherrer B, et al. Multimodal MRI segmentation of ischemic stroke lesions. *Conf Proc IEEE Eng Med Biol Soc* 2007; 2007: 1595–1598.

27. Bakker CJ, Hartkamp MJ and Mali WP. Measuring blood flow by nontriggered 2D phase-contrast MR angiography. *Magn Reson Imaging* 1996; 14: 609–614.

28. Vestergaard MB, Lindberg U, Aachmann-Andersen NJ, et al. Comparison of global cerebral blood flow measured by phase-contrast mapping MRI with 15 O-H2 O positron emission tomography. *J Magn Reson Imaging* 2017; 45: 692–699.

29. Torack RM, Alcala H, Gado M, et al. Correlative assay of computerized cranial tomography CCT, water content and specific gravity in normal and pathological postmortem brain. *J Neuropathol Exp Neurol* 1976; 35: 385–392.

30. Jain V, Langham MC and Wehrli FW. MRI estimation of global brain oxygen consumption rate. *J Cereb Blood Flow Metab* 2010; 30: 1598–1607.

31. Rodgers ZB, Jain V, Englund EK, et al. High temporal resolution MRI quantification of global cerebral metabolic rate of oxygen consumption in response to apneic challenge. *J Cereb Blood Flow Metab* 2013; 33: 1514–1522.

32. Vestergaard MB and Larsson HB. Cerebral metabolism and vascular reactivity during breath-hold and hypoxic challenge in freedivers and healthy controls. *J Cereb Blood Flow Metab* 2019; 39: 834–848.

33. Mima T, Yanagisawa M, Shigeno T, et al. Endothelin acts in feline and canine cerebral arteries from the adventitial side. *Stroke* 1989; 20: 1553–1556.

34. Koseki C, Imai M, Hirata Y, et al. Autoradiographic localization of [125I]-endothelin-1 binding sites in rat brain. *Neurosci Res* 1989; 6: 581–585.

35. Robinson MJ, Macrae IM, Todd M, et al. Reduction of local cerebral blood flow to pathological levels by endothelin-1 applied to the middle cerebral artery in the rat. *Neurosci Lett* 1990; 118: 269–272.

36. Hughes PM, Anthony DC, Ruddin M, et al. Focal lesions in the rat central nervous system induced by endothelin-1. *J Neuropathol Exp Neurol* 2003; 62: 1276–1286.

37. Kleinschnitz C, Fluri F and Schuhmann M. Animal models of ischemic stroke and their application in clinical research. *Drug Des Devel Ther* 2015; 9: 3445–3454.

38. Clozel M and Clozel JP. Effects of endothelin on regional blood flows in squirrel monkeys. *J Pharmacol Exp Ther* 1989; 250: 1125–1131.

39. Kadel KA, Heistad DD and Faraci FM. Effects of endothelin on blood vessels of the brain and choroid plexus. *Brain Res* 1990; 518: 78–82.

40. García JL, Gómez B, Monge L, et al. Endothelin action on cerebral circulation in unanesthetized goats. *Am J Physiol* 1991; 261: R581–R587.

41. Amin FM, Asghar MS, Guo S, et al. Headache and prolonged dilatation of the middle meningeal artery by PACAP38 in healthy volunteers. *Cephalalgia* 2012; 32: 140–149.

42. Asghar MS, Hansen AE, Kapijimpanga T, et al. Dilation by CGRP of middle meningeal artery and reversal by sumatriptan in normal volunteers. *Neurology* 2010; 75: 1520–1526.

43. Brothers RM and Zhang R. CrossTalk opposing view: the middle cerebral artery diameter does not change during alterations in arterial blood gases and blood pressure. *J Physiol* 2016; 594: 4077–4079.

44. Hoiland RL and Ainslie PN. CrossTalk proposal: the middle cerebral artery diameter does change during alterations in arterial blood gases and blood pressure. *J Physiol* 2016; 594: 4073–4075.

45. Giller CA, Bowman G, Dyer H, et al. Cerebral arterial diameters during changes in blood pressure and carbon dioxide during craniotomy. *Neurosurgery* 1993; 32: 737–741; discussion 741–2.

46. Serrador JM, Picot PA, Rutt BK, et al. MRI measures of middle cerebral artery diameter in conscious humans during simulated orthostasis. *Stroke* 2000; 31: 1672–1678.

47. Haynes WG, Ferro CJ, O'Kane KP, et al. Systemic endothelin receptor blockade decreases peripheral vascular resistance and blood pressure in humans. *Circulation* 1996; 93: 1860–1870.

48. Vergouwen MDI, Algra A and Rinkel GJE. Endothelin receptor antagonists for aneurysmal subarachnoid hemorrhage. *Stroke* 2012; 43: 2671–2676.

49. Charles AC and Baca SM. Cortical spreading depression and migraine. *Nat Rev Neurol* 2013; 9: 637–644.

50. Dreier JP. Endothelin-1 potently induces Leao's cortical spreading depression in vivo in the rat: a model for an endothelial trigger of migrainous aura? *Brain* 2002; 125: 102–112.

51. Kleeberg J. ET-1 induces cortical spreading depression via activation of the ETA receptor/phospholipase C pathway in vivo. *Am J Physiol Heart Circ Physiol* 2003; 286: H1339–H1346.

52. Dreier JP, Kleeberg J, Alam M, et al. Endothelin-1-induced spreading depression in rats is associated with a microarea of selective neuronal necrosis. *Exp Biol Med* 2007; 232: 204–213.

53. Gillet JL, Donnet A, Lausecker M, et al. Pathophysiology of visual disturbances occurring after foam sclerotherapy. *Phlebology* 2010; 25: 261–266.

54. Frullini A, Barsotti MC, Santoni T, et al. Significant endothelin release in patients treated with foam sclerotherapy. *Dermatol Surg* 2012; 38: 741–747.

55. Lindholt M, Petersen KA, Tvedskov JF, et al. Lack of effect of norepinephrine on cranial haemodynamics and headache in healthy volunteers. *Cephalalgia* 2009; 29: 384–387.

56. Antonova M, Wienecke T, Olesen J, et al. Pro-inflammatory and vasoconstricting prostanoid PGF2α causes no headache in man. *Cephalalgia* 2011; 31: 1532–1541.